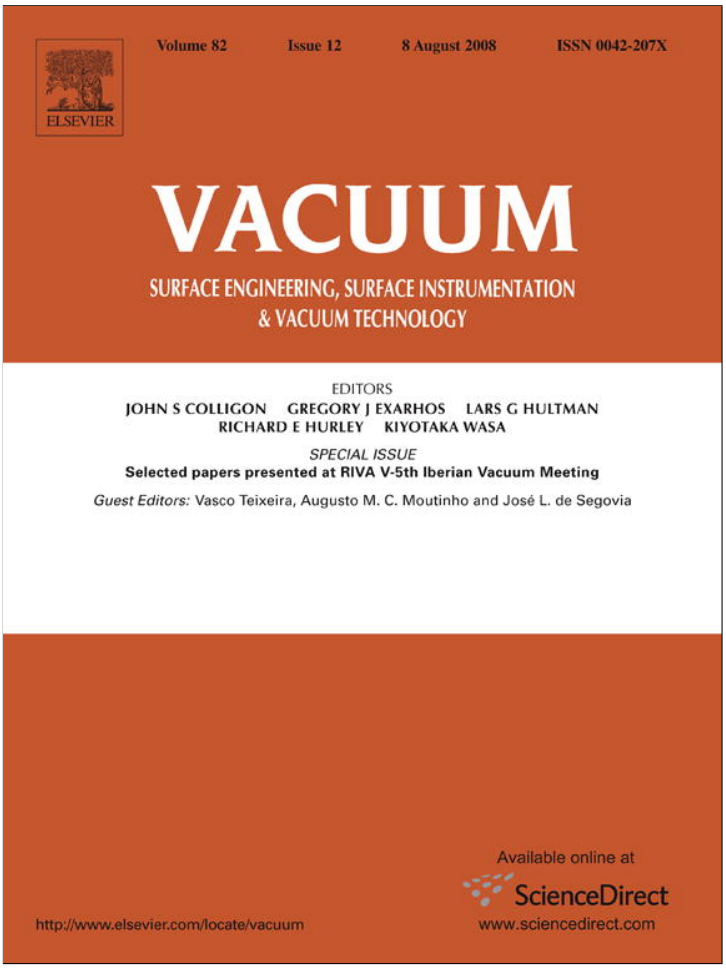

Vacuum 82 (2008) 1400–1403

Contents lists available at ScienceDirect

Vacuum

journal homepage: www.elsevier.com/locate/vacuum

Annealing effects on the structural properties of IrO_2 thin films

Hyoun Woo Kim*, Seung Hyun Shim, Ju Hyun Myung, Chongmu Lee

School of Materials Science and Engineering, Inha University, Incheon 402-751, Republic of Korea

Keywords:
IrO_2
Structural properties
Thermal annealing

A B S T R A C T

We have demonstrated the structural and morphological changes of iridium oxide (IrO_2) films by the thermal annealing process. We have characterized the samples by using the X-ray diffraction (XRD), scanning electron microscopy (SEM), and energy dispersive X-ray spectroscopy (EDX). The Ir-related XRD peaks predominantly appeared after the thermal annealing at 750–1000 °C. SEM images revealed that the films became quite uneven in thickness by annealing at 750 °C, whereas island-like structures were found to agglomerate on substrate surfaces by annealing at 1000 °C. From EDX and XRD analysis, we suggested that the agglomerated structures mainly consisted of Ir phase.

1. Introduction

Iridium oxide (IrO_2) is a transition metal oxide that exhibits metallic conductivity at room temperature and possesses interesting electrochemical properties that makes it a very attractive material for many applications such as optical switching layers in electrochromic devices [1], pH-sensing materials [2,3], and durable electrode material for chlorine or oxygen evolution [4]. In addition, IrO_2 is a promising conducting oxide for use as an electrode material in ferroelectric capacitors in nonvolatile memories applications [5] because it combines attractive properties, such as low resistivity [6], an excellent diffusion barrier, chemical inertia towards silicon at temperatures as high as 800 °C, and is effective in eliminating the polarization fatigue observed in ferroelectric $Pb(Zr_xTi_{1-x})O_3$ thin film capacitors. Therefore, various methods have been used to prepare IrO_2 films including thermal oxidation [7], anodic oxidation [8], reactive sputtering [9], sol–gel process [4], and pulsed laser deposition (PLD) [10].

Although an IrO_2 layer needs to be used in various applications such as high temperature VLSI environments, to the best of the authors' knowledge, there is no experimental data reported on its annealing behavior of the films. In this study, we investigated the effects of annealing on IrO_2 films prepared by sputtering, with respect to their structural changes as a function of the annealing temperature.

2. Experimental

First, a 100 nm of thermal oxide layer was formed on Si (100) wafers. Subsequently, a thin adhesion layer of Ti (<10 nm) has been sputtered on top of SiO_2. A 200-nm IrO_2 thin film was then deposited by DC magnetron sputtering using an Ir target in a Ar/O_2 atmosphere. The substrate temperature, the DC power, and pressure for IrO_2 deposition was fixed at 250 °C, 750 W, and 6 mTorr, respectively, being an actual deposition condition for IrO_2 electrode materials in memory devices. After film deposition, the samples were annealed in a quartz tube furnace at temperatures ranging from 350 to 1000 °C in an Ar ambient atmosphere for 1 h. The Ar flow rate was set at 0.5 standard liters per min (slm).

The structural characteristics of the samples were examined by glancing angle X-ray diffraction (XRD; Philips, CM20T, 200 kV) with an incident angle of 0.5°, using $CuK\alpha_1$ radiation ($\lambda = 0.154056$ nm). In glancing angle studies, measurements were made at a fixed low glancing angle of the primary beam to maximize the signals from the layers and minimize the substrate reflections. The 3-dimensional film morphology was examined using scanning electron microscopy (SEM; Hitachi S-4200) with energy dispersive X-ray (EDX) spectroscopy installed. EDX measurements were carried out to identify the chemical elements of the as-prepared products.

3. Results and discussion

Fig. 1a–e shows the XRD patterns, respectively, of the as-deposited IrO_2 films, and those annealed at 350, 500, 750, and 1000 °C. The as-deposited IrO_2 film was almost amorphous (Fig. 1a). With the 350- and 500 °C-annealed IrO_2 films (Fig. 1b and c), the XRD peaks were indexed to the (110), (200) and (211) diffraction

* Corresponding author.
E-mail address: hwkim@inha.ac.kr (H.W. Kim).

0042-207X/$ – see front matter © 2008 Elsevier Ltd. All rights reserved.
doi:10.1016/j.vacuum.2008.03.004

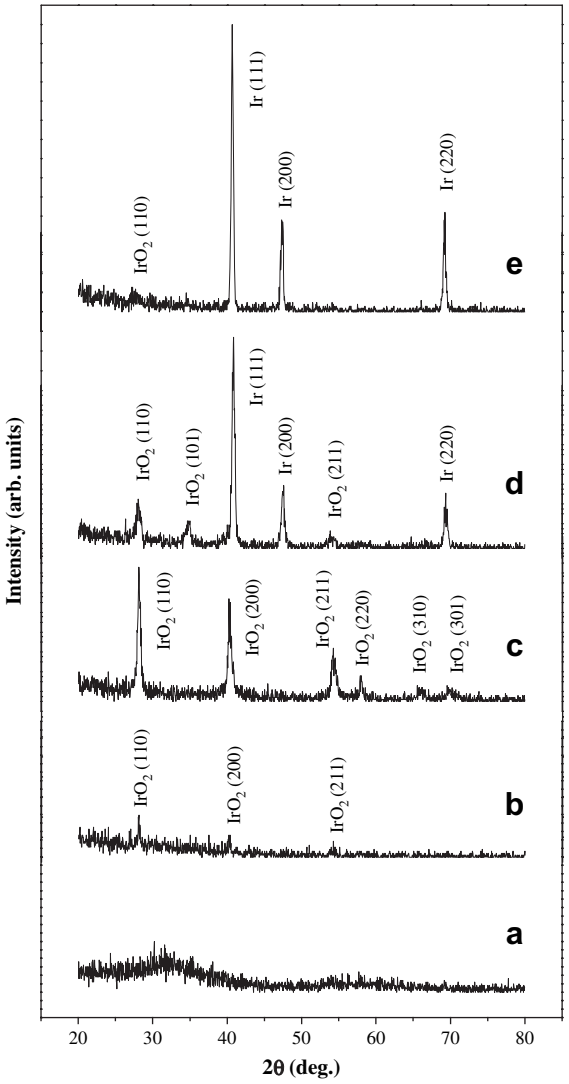

Fig. 1. XRD spectra for (a) as-deposited and annealed IrO_2 films at (b) 350 °C, (c) 500 °C, (d) 750 °C, and (e) 1000 °C.

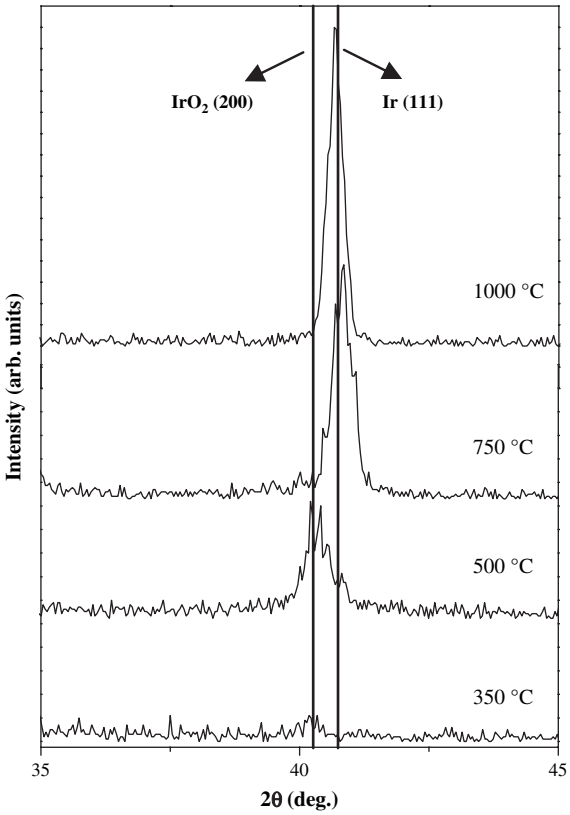

Fig. 2. XRD patterns for annealed samples between 35 and 45° (2θ).

peaks for tetragonal IrO_2 (JCPDS 15-0870). It should be noted that additional weak lines indexed to the (220), (310), and (301) diffraction peaks of tetragonal IrO_2 appeared in the films annealed at 500 °C. XRD analysis also reveals that the Ir phase can be found in the 750–1000 °C-annealed samples, from the existence of the (200) diffraction peak for cubic Ir (JCPDS 06-0598) (Fig. 1d and e). Because the peak position of the Ir (111) peak is very close to the IrO_2 (200) peak, these peaks were enlarged for clarity (Fig. 2). Fig. 2 shows that the Ir (111) peak of the 750–1000 °C-annealed sample replaces the IrO_2 (200) peak of the 350–500 °C-annealed samples.

Therefore, when annealed at 750 °C, apart from the (110), (101), and (211) peaks corresponding to IrO_2 phase, the relatively strong lines were found to coincide with the (111), (200), and (220) peaks of cubic Ir (JCPDS 06-0598) (Fig. 1d). When annealed at 1000 °C, there were three strong lines corresponding to the Ir (111), Ir (200), and Ir (220) peaks, with only trace amounts of the IrO_2 (110) peak (Fig. 1e). Similar XRD spectra were obtained from the Ir films deposited by reactive PLD [11]. In case of PLD experiments, the oxygen ambient pressure has been varied, revealing that relatively low and high oxygen pressured process tended to generate Ir and IrO_2 phases, respectively [11], whereas the sputtering in our experiments has been carried out via a relatively O_2-abundant process, generating the IrO_2 phases. Furthermore, the (111) orientation may be favored in Ir films, most likely because the (111) planes are close-packed in the face centered cubic Ir structure, which agrees with the strong (111) peaks of the XRD spectrum in Fig. 1d and e.

Fig. 3a–c shows cross-sectional SEM images of the thin films annealed at 500, 750 and 1000 °C, respectively. The as-deposited samples and those annealed up to 500 °C exhibited a smooth surface morphology. On the other hand, the films become quite uneven in thickness after thermal annealing at 750 °C. The sample annealed at 1000 °C had a cluster-like structure on the substrate. Accordingly, annealed films at 750–1000 °C present serious degradation as evident on the SEM images. We have calculated the grain size of 1000 °C-annealed sample. The mean grain diameter L_{hkl}, which is perpendicular to the (hkl) plane, can be calculated using the Debye–Scherer formula $L_{hkl} = 0.9\lambda/(B_{hkl}\cos\theta_B)$, where λ is the X-ray wavelength (0.154 nm), θ_B is the Bragg diffraction angle, and B_{hkl} is the peak width at half maximum of the (hkl) diffraction peak. In the present analysis, the recognizable Ir diffraction peaks corresponding to (111), (200), and (220) indices are extracted (Fig. 1e). After calculating the grain diameters perpendicular to the crystalline planes with different indices (i.e. $L_{111} = 24.2$ nm, $L_{200} = 24.8$ nm, and $L_{220} = 30.2$ nm), we obtained the value of the average grain size, which is a weighted average considering the relative XRD peak intensity (Average grain size $D = \Sigma(\alpha_{hkl}L_{hkl})$; L_{hkl} is XRD grain diameter which is perpendicular to the (hkl) plane and orientation parameter $\alpha_{hkl} = (I_{hkl}/I^*_{hkl})/(\Sigma\ I_{hkl}/I^*_{hkl})$, where I_{hkl} is the measured intensity of (hkl) peak and I^*_{hkl} is the standard intensity of the JCPDS standard powder diffraction data of Ir (06-0598)). Accordingly, the average grain size of Ir island structures is estimated to be about 26.4 nm. By comparing with the dimension of Ir islands in Fig. 3c (~ several hundreds nanometers), we reveal that the islands are polycrystalline in nature.

Fig. 4a–c shows the plan-view SEM images of the thin films, respectively, which were annealed at 500, 750 and 1000 °C,

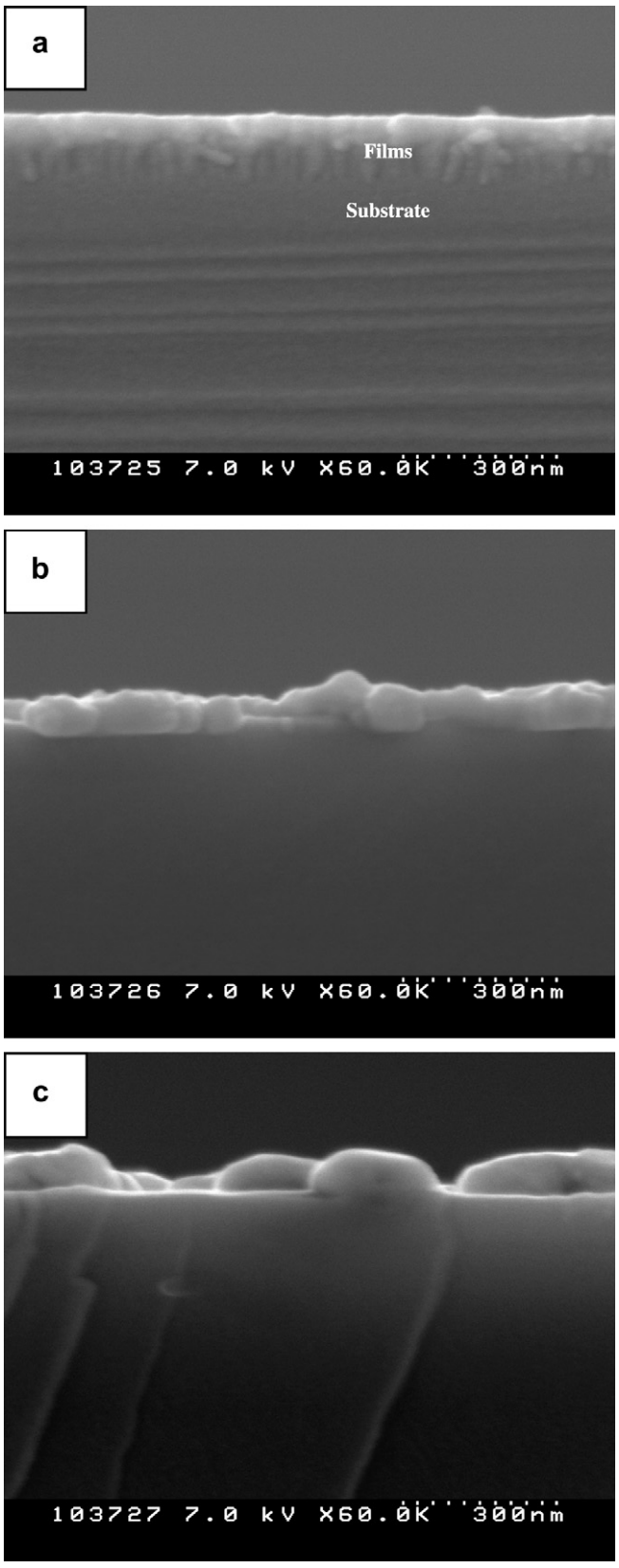

Fig. 3. Cross-sectional SEM images of IrO_2 films annealed at (a) 500 °C, (b) 750 °C, and (c) 1000 °C.

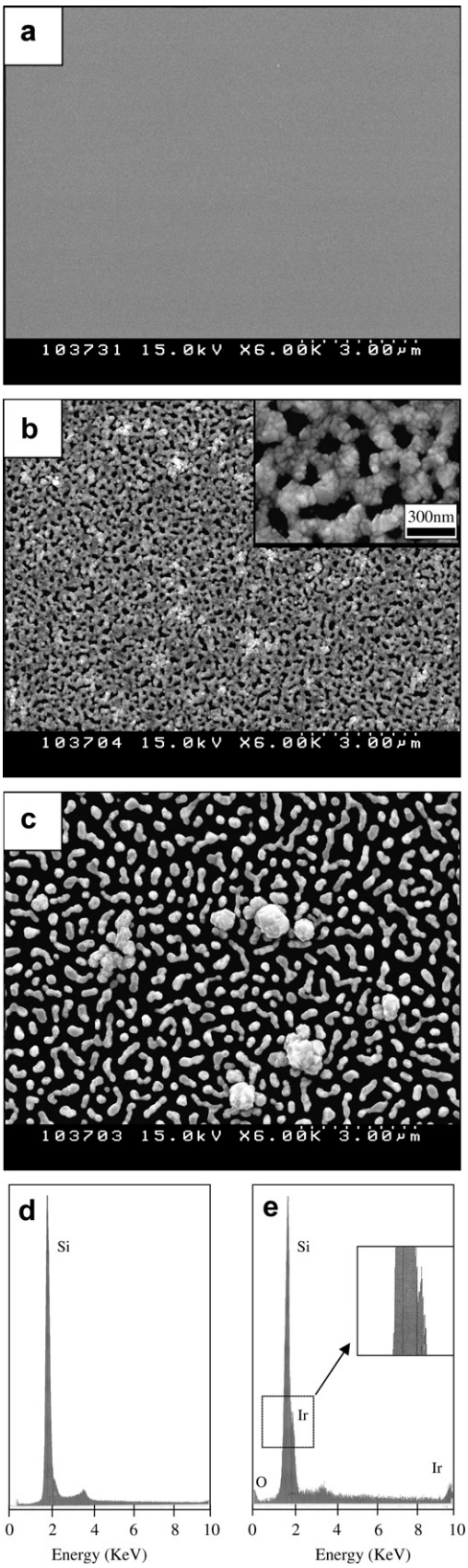

Fig. 4. Plan-view SEM images of IrO_2 films annealed at (a) 500 °C, (b) 750 °C, and (c) 1000 °C. The top right inset in Fig. 4b shows an enlarged image. EDS spectra corresponding to the (d) blackened and (e) whitened region in Fig. 4c.

respectively. While the smooth film surfaces can be clearly seen in the 500 °C-annealed sample, severe island formation was observed on the substrate surface of the 1000 °C-annealed sample. The 750 °C-annealed sample may represent an intermediate state. It is noteworthy that this island-like morphology can be very useful in the fabrication of capacitor structures in DRAM and/or FRAM devices, in which the IrO_2 islands function as bottom electrodes. Since each IrO_2 island stands for the bottom electrode of one capacitor component, the neighbouring IrO_2 island should be disconnected. In the present scheme, formation of island-like IrO_2 automatically separates neighbouring bottom electrode structures. Therefore, we do not need additional photolithography and etching processes.

Fig. 4d and e, respectively, shows the EDX spectrum corresponding to the blackened and whitened regions in Fig. 4c, respectively. While EDX analysis made on the blackened region demonstrates that the elements mainly consist of Si, the elements corresponding to the island-like structures (i.e. blackened region) are composed of Si and Ir, with only trace amounts of O. It is believed that the Si-related peaks are from the substrate underneath or in the vicinity of the islands. Although the exact chemical composition is not known, it is possible that the island-like structure comprises of Ir with trace amounts of O.

From the above observations, we suggest that the morphological changes with increasing the annealing temperatures may be the result of the volume contraction mainly due to the decomposition and reduction of IrO_2 films. After thermal annealing at 1000 °C, the material tends to coagulate to form island-like structures. More study is currently underway in order to reveal the detailed mechanisms.

4. Conclusions

In summary, for the first time we investigated the influence of thermal annealing on iridium oxide (IrO_2) films deposited on silicon dioxide (SiO_2)/Si substrates. XRD analysis revealed that the relative intensities of the Ir peaks compared with the IrO_2 peaks increased after thermal annealing at 750–1000 °C. SEM images suggest that an island-like structures agglomerate on substrate surfaces after annealing at 1000 °C. EDX suggested that the island-like structures consisted mainly of Ir with trace amounts of O.

Acknowledgements

This work was supported by Inha Research Fund 2006.

References

[1] Cogan SF, Plante TD, Mcfadden RS, Rauh RD. Sol Energy Mater 1987;16:371.
[2] Fog A, Buck RP. Sensor Actuator 1984;5:137.
[3] Katsube T, Lauks I, Zemel JN. Sensor Actuator 1982;2:399.
[4] Osaka A, Takatsuna T, Miura Y. J Non-Cryst Solids 1994;178:313.
[5] Nakamura T, Nakao Y, Kamisawa A, Takasu H. Appl Phys Lett 1994;65:1522.
[6] Ryden WD, Lawson AW, Sartain CC. Phys Rev B 1970;1:1494.
[7] Sato Y. Vacuum 1980;41:1198.
[8] Beni G, Shay JL. Appl Phys Lett 1978;33:567.
[9] Hackwood S, Dayem AH, Beni G. Phys Rev B 1982;26:471.
[10] El Khakani MA, Chaker M, Gat E. Appl Phys Lett 1996;69:2027.
[11] El Khakani MA, Chaker M. Thin Solid Films 1998;335:6.